The composition of the microbiota modulates allograft rejection

Yuk Man Lei,[1] Luqiu Chen,[1] Ying Wang,[1] Andrew T. Stefka,[2] Luciana L. Molinero,[1] Betty Theriault,[3] Keston Aquino-Michaels,[4] Ayelet S. Sivan,[2] Cathryn R. Nagler,[2] Thomas F. Gajewski,[2] Anita S. Chong,[5] Caroline Bartman,[1] and Maria-Luisa Alegre[1]

[1]Section of Rheumatology, Department of Medicine, [2]Department of Pathology, [3]Gnotobiotic Research Animal Facility, [4]Section of Genetic Medicine, Department of Medicine, and [5]Section of Transplantation, Department of Surgery, University of Chicago, Chicago, Illinois, USA.

Transplantation is the only cure for end-stage organ failure, but without immunosuppression, T cells rapidly reject allografts. While genetic disparities between donor and recipient are major determinants of the kinetics of transplant rejection, little is known about the contribution of environmental factors. Because colonized organs have worse transplant outcome than sterile organs, we tested the influence of host and donor microbiota on skin transplant rejection. Compared with untreated conventional mice, pretreatment of donors and recipients with broad-spectrum antibiotics (Abx) or use of germ-free (GF) donors and recipients resulted in prolonged survival of minor antigen–mismatched skin grafts. Increased graft survival correlated with reduced type I IFN signaling in antigen-presenting cells (APCs) and decreased priming of alloreactive T cells. Colonization of GF mice with fecal material from untreated conventional mice, but not from Abx-pretreated mice, enhanced the ability of APCs to prime alloreactive T cells and accelerated graft rejection, suggesting that alloimmunity is modulated by the composition of microbiota rather than the quantity of bacteria. Abx pretreatment of conventional mice also delayed rejection of major antigen–mismatched skin and MHC class II–mismatched cardiac allografts. This study demonstrates that Abx pretreatment prolongs graft survival, suggesting that targeting microbial constituents is a potential therapeutic strategy for enhancing graft acceptance.

Introduction

Although solid organ transplantation is the only cure for end-stage organ failure, recognition of the transplanted tissue as foreign invariably leads, in the absence of immunosuppression, to its acute rejection in a T cell–dependent manner. The kinetics of graft rejection mostly depend on the extent of genetic disparities between the donor and the recipient, as allelic differences can result in protein polymorphisms recognized by alloreactive host T cells. Whether environmental factors modulate the intensity of the alloresponse is not clear.

We have previously reported that infections with *Listeria monocytogenes* or *Staphylococcus aureus* at the time of transplantation can increase alloreactivity and prevent the induction of transplantation tolerance by costimulation-blocking agents (1, 2). This led us to consider whether more ubiquitous bacteria such as the commensal communities that colonize donors and recipients might also modulate alloreactivity. Indeed, it is now well established that the microbiota can modify local and distal immune responses (3), thus raising the possibility that it might fine-tune alloreactivity. Several lines of evidence indirectly support this hypothesis. First, organs colonized with bacteria such as lung and intestine have poorer outcomes than organs considered sterile such as heart and kidney (Organ Procurement and Transplantation Network (OPTN), https://optn.transplant.hrsa.gov/data/; Scientific Registry of Transplant Recipients (SRTR), http://www.srtr.org/, December 2012). Second, the survival of minor antigen–mismatched skin grafts is prolonged when both donor and recipient lack MyD88-dependent TLR signaling (4), although the relative contribution of damage- versus microbe-associated molecular patterns has not been elucidated. Third, emerging clinical literature suggests that acute rejection of intestine and lung may be associated with shifts in bacterial composition (5, 6), although it is not yet clear whether such shifts are a cause or a consequence of acute rejection. Therefore, direct assessment of the role of the microbiota on alloimmunity is needed.

▶ Related Commentary: p. 2422

Authorship note: C. Bartman and M.L. Alegre are co–last authors.
Conflict of interest: The authors have declared that no conflict of interest exists.
Submitted: November 2, 2015; **Accepted:** May 4, 2016.
Reference information: *J Clin Invest*. 2016;126(7):2736–2744. doi:10.1172/JCI85295.

Results

Minor antigen–mismatched skin graft survival was prolonged in antibiotic-pretreated mice. To determine the consequence of reduced bacterial diversity on allograft outcome, 6- to 8-week-old male and female purchased C57BL/6 (B6) mice were left untreated or received a daily gavage of antibiotics (Abx) for 10 days. Skin from male donors was transplanted onto the flanks of female mice 1 day later, and recipients did not receive further Abx treatment. Abx-pretreated recipients of skin grafts from Abx-pretreated donors displayed prolonged skin allograft survival (mean survival time [MST] = 53 ± 23 days) compared with controls (MST = 27 ± 12 days) (Figure 1A). Similar results were obtained when comparing untreated and Abx-pretreated in-house–bred littermates derived from the same maternal lineage to minimize microbiota differences between groups prior to treatment (Supplemental Figure 1A; supplemental material available online with this article; doi:10.1172/JCI85295DS1). In contrast, Abx pretreatment of

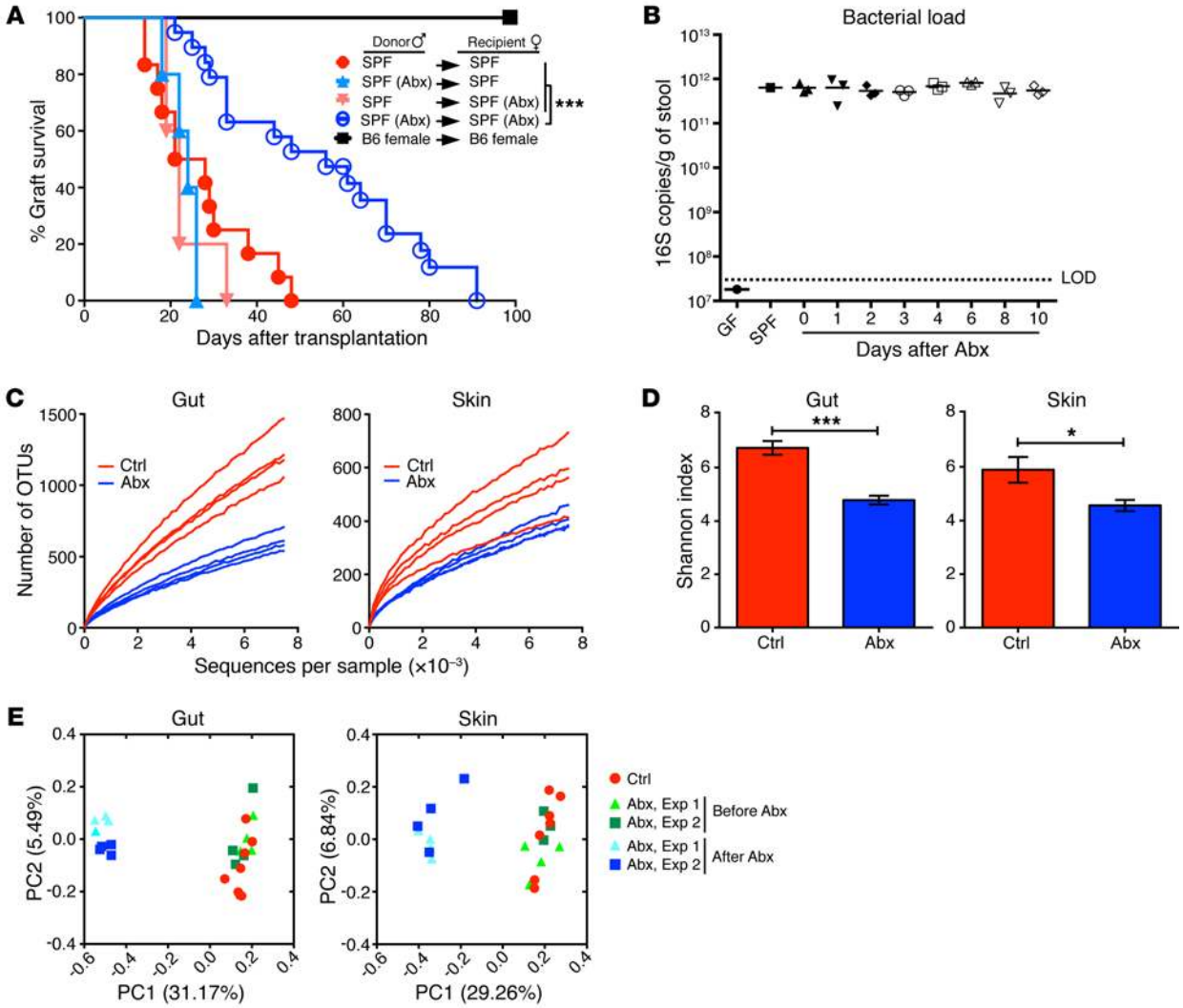

Figure 1. Abx pretreatment results in prolonged skin graft survival and reduced bacterial diversity. (**A**) B6 females untreated or pretreated for 10 days with Abx received a skin graft from B6 males untreated or pretreated for 10 days with Abx. SPF → SPF, n = 12; SPF (Abx) → SPF, n = 5; SPF → SPF (Abx), n = 5; Abx → Abx, n = 19; syngeneic, n = 5. log-rank test. (**B**) Bacterial load by qPCR in fecal samples of GF and SPF B6 females at the indicated time points after initiation of Abx treatment. n = 3 (1 SPF and 1 GF samples shown for reference). LOD, level of detection. (**C**–**E**) Bacterial DNA was isolated from gut and skin of female SPF controls and age-matched mice on day 10 of Abx treatment and was analyzed by high-throughput sequencing. Data are displayed as richness (**C**), diversity (**D**), and PCA (**E**). Each line (**C**) and dot (**B** and **E**) represents an individual mouse. PC1, principal component 1; Exp, experiment. Bars (**D**) represent the mean ± SEM of 4 mice per group. (**C**–**E**) Results are representative of 4 experiments with n = 3–4. *P < 0.05; ***P < 0.001, Student's t test.

donors or recipients alone did not delay rejection (Figure 1A), indicating that Abx-induced changes in both the donor skin and the recipient mice are required for improved graft survival.

To understand the changes that had occurred in the microbiota prior to transplantation, bacterial DNA was extracted from tail skin and fecal samples of female hosts. This Abx regimen in adult mice did not reduce overall fecal bacterial burden, as determined by qPCR using universal primers for the 16S rRNA gene (Figure 1B), in contrast with the reduced bacterial load that occurs when a similar regimen is started in 2-week-old mice prior to weaning (7). However, 10-day Abx pretreatment resulted in significantly reduced bacterial richness and diversity on the day of transplantation (Figure 1, C and D) in both fecal and skin samples, as determined by 16S rRNA sequencing using the MiSeq platform. Furthermore, principal component analysis (PCA) showed that microbial communities of fecal and skin samples on day 10 of Abx pretreatment clustered separately from those of the control and the pretreatment groups (Figure 1E). In particular, Abx-pretreated mice had a relative expansion of *Lactobacillales* in their feces and a reduction of *Clostridiales* in both feces and skin (Supplemental Figure 1, B and C). Thus, Abx pretreatment changed the composition of the microbiota, but not the overall bacterial load.

Minor antigen–mismatched skin allograft survival was prolonged in GF mice. As a second approach to testing the role of the microbiota on graft outcome, we used germ-free (GF) mice, devoid of live bacteria, and transplanted them in a biological safety cabinet in the gnotobiotic facility using sterile techniques (Figure 2A and ref. 8). GF female recipients of GF male skin transplants also displayed prolonged graft survival when compared with specific pathogen–free (SPF) mice transplanted in a sterile manner (Figure 2B). This

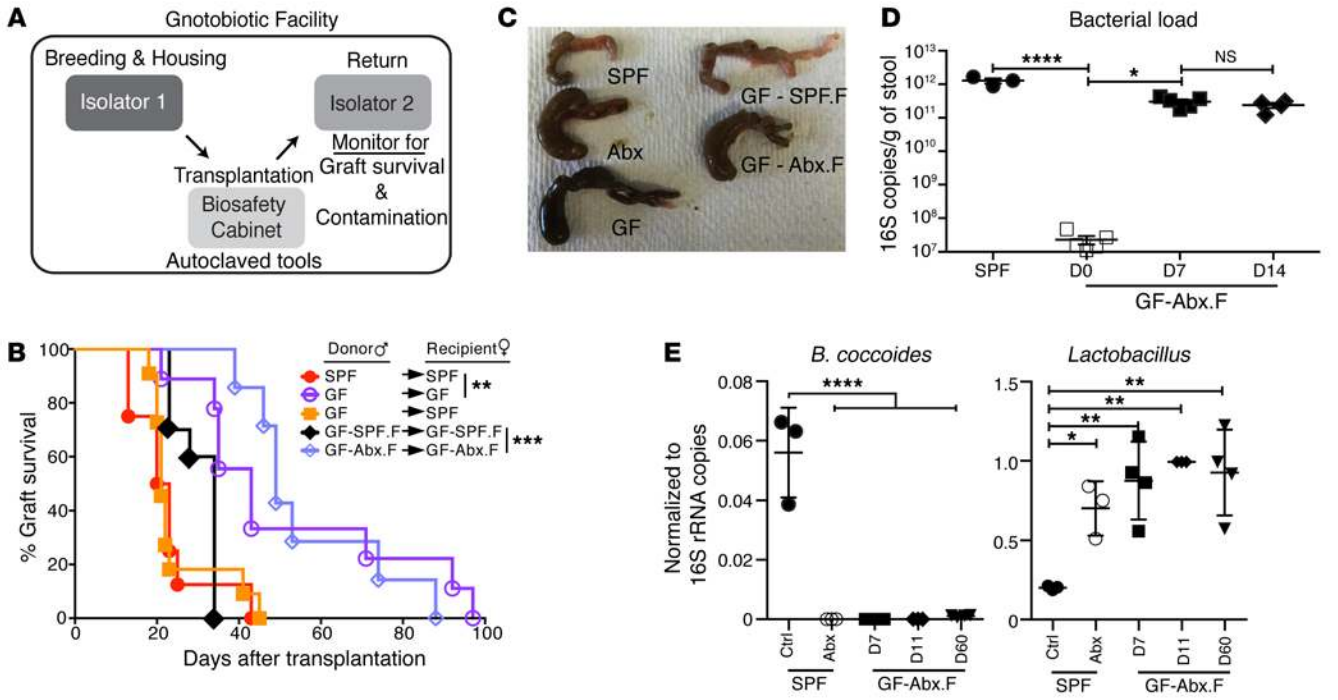

Figure 2. GF mice display prolonged skin graft survival. (**A**) Schematics of transplantation in the gnotobiotic facility. (**B**) B6 female SPF, GF, and GF mice gavaged with PBS-diluted fecal material from SPF mice (GF-SPF.F) or Abx-pretreated SPF mice (GF-Abx.F) 5 to 7 days prior, were transplanted with male skin grafts from the indicated donors. SPF → SPF, $n = 8$; GF → GF, $n = 8$; GF → SPF, $n = 11$; GF-SPF.F → GF-SPF.F, $n = 10$; GF-Abx.F → GF-Abx.F, $n = 7$. log-rank test. (**C**) Representative cecum appearance at day 7 after gavage. (**D**) qPCR of 16S rRNA gene to assess bacterial load in SPF, GF, and GF-Abx.F mice before and after gavage. $n = 3$–5. One-way ANOVA. (**E**) Normalized abundance of *B. coccoides* and *Lactobacillus* spp. as determined by qPCR in feces of SPF, 10-day Abx-treated SPF mice, and GF-Abx.F mice after fecal gavage. $n = 3$–5. One-way ANOVA. Data are representative of 2 experiments (**D**–**F**) or combined from 2 to 3 experiments (**B**). (**B** and **E**) Data represent the mean ± SEM. $^*P < 0.05$; $^{**}P < 0.01$; $^{***}P < 0.001$; $^{****}P < 0.0001$.

was not due to a reduced susceptibility of GF skin to rejection, as GF grafts were rejected as promptly as SPF grafts by SPF mice (Figure 2B). To test the causal role of the microbiota, GF mice received a gavage with feces from SPF mice 5 to 7 days prior to transplantation (GF-SPF.F). Although the microbial communities that established in the intestine of GF-SPF.F mice differed from those in the donor fecal samples (Supplemental Figure 2, A and B), restoration of the microbiota was sufficient to accelerate rejection (Figure 2B), indicating that prolonged graft survival in sterile GF mice is due at least in part to their lack of microbiota.

To determine whether all microbial communities accelerated graft rejection, GF mice were gavaged with feces from Abx-pretreated SPF mice (GF-Abx.F) prior to transplantation. In contrast with GF-SPF.F mice, GF-Abx.F mice did not display faster rejection than GF mice (Figure 2B) and their cecal appearance remained enlarged, as is typical of GF mice (ref. 9 and Figure 2C), despite a bacterial load close to that in SPF mice (Figure 2D). The dysbiosis induced by Abx pretreatment in the fecal donors was transferred and remained stably established in GF-Abx.F recipients that were not exposed to other environmental bacteria, as supported by the persistent contraction of *Blautia coccoides* (formerly classified as *Clostridium coccoides*; ref. 10) and expansion of *Lactobacillus* spp. (Figure 2E), although their total bacterial communities were still distinct from those in the donor fecal samples (Supplemental Figure 2, A and B). Interestingly, fecal transfer into GF mice not only resulted in intestinal, but also skin colonization (Supplemental Figure 2, A and B), such that whether it is the gut and/or skin microbiota that influences skin graft outcome remains to be elucidated.

Abx pretreatment resulted in reduced alloimmunity. To investigate whether improved graft survival in Abx-pretreated mice was due to reduced alloimmunity, we analyzed graft-infiltrating leukocytes isolated on day 10 after transplantation. Abx pretreatment was associated with a reduced percentage of $CD4^+$ T cells and fewer IFN-γ–producing cells among them (Figure 3, A–C). To test whether the reduced percentage of intragraft effector $CD4^+$ T cells was due to diminished expansion of alloreactive T cells, H-Y–specific $CD45.1^+$ congenic $CD4^+$ TCR/RAG-KO-Tg (Marilyn) T cells were CFSE-labeled and adoptively transferred into 10-day–Abx–pretreated female recipients 1 day prior to transplantation with skin grafts from Abx-pretreated male donors. Marilyn T cells isolated 4 days later from the skin graft draining LNs (dLNs), the site of initial T cell priming after skin transplantation (11), displayed reduced proliferation in Abx-pretreated mice compared with that in untreated hosts (Figure 3, D and E). Thus, Abx pretreatment triggered reduced priming of graft-reactive T cells, supporting the conclusion that the microbiota that associates with SPF B6 mice in our colony promotes the activation of alloreactive T cells and/or that Abx pretreatment promotes a microbial community that reduces alloreactivity.

In order to modulate T cell priming, microbial signals might directly or indirectly affect T cells, antigen-presenting cells

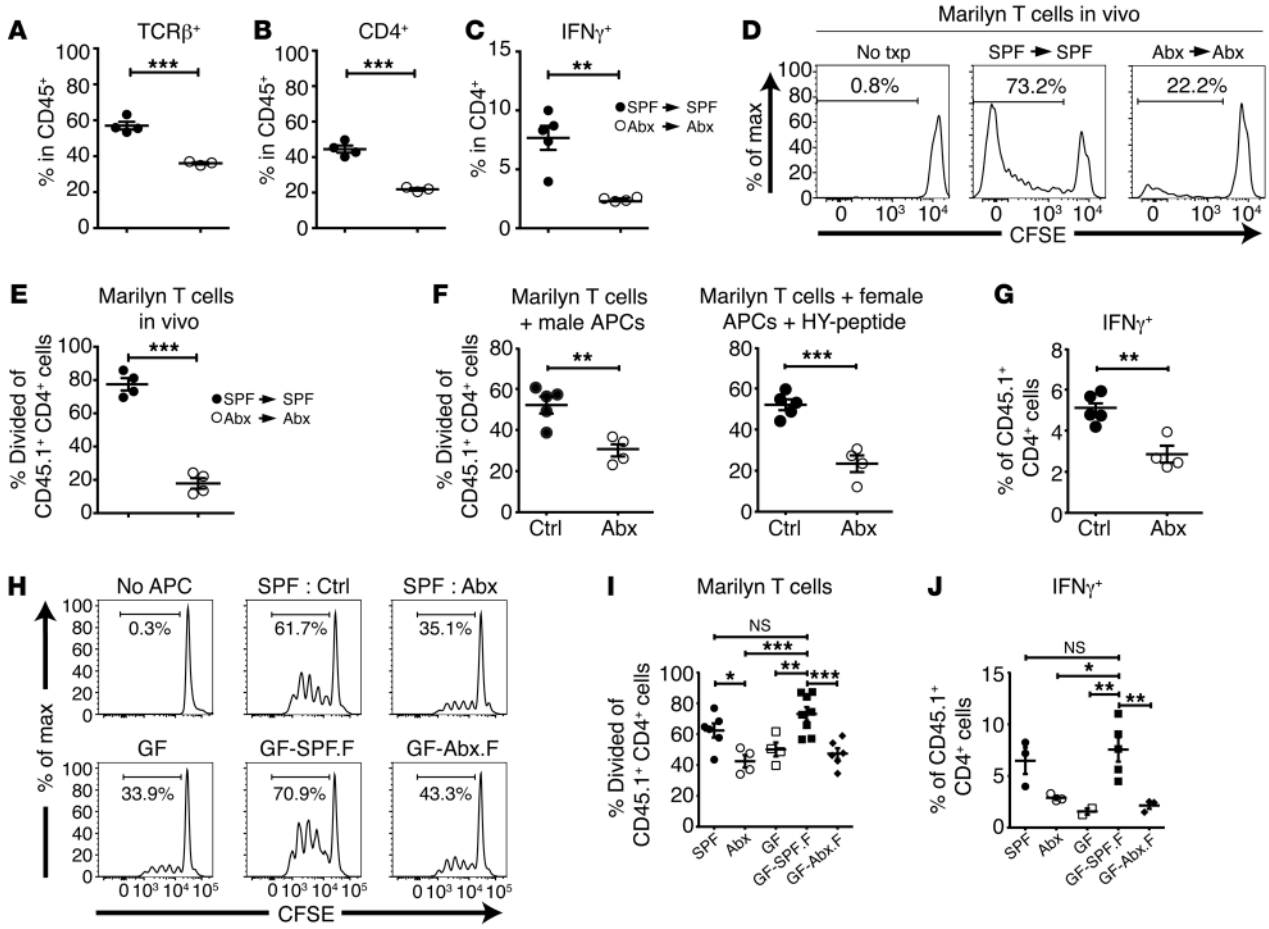

Figure 3. Abx pretreatment and GF status result in reduced allogeneic T cell priming. (**A**–**C**) Graft-infiltrating cells were isolated from control and Abx-pretreated SPF mice on day 10 after transplantation for flow cytometric analysis to determine the percentage of TCR-β+ (**A**) or CD4+ (**B**) cells among CD45+ cells and the percentage of IFN-γ–producing cells (**C**) among PMA/ionomycin-stimulated CD4+ cells. (**D** and **E**) Congenic Marilyn T cells were labeled with CFSE and transferred (10^6 cells/mouse) into SPF female recipients 1 day prior to transplantation with male skin grafts; donors and recipients were both untreated or both Abx pretreated. Mice were sacrificed 4 days after transplantation, and cells were isolated from the graft dLNs for analysis of CFSE dilution. Representative plots (**D**) and quantitation (**E**) of divided Marilyn T cells. (**F** and **G**) APCs from skin dLN cells were isolated from control or 10-day Abx-pretreated SPF B6 males or females and cultured with CFSE-labeled T cells from naive Marilyn females. (**F**) Quantitation of CFSE dilution in Marilyn-gated T cells on day 4 of culture. (**G**) Percentage of IFN-γ+ cells among Marilyn T cells after a 3-day culture and following restimulation with PMA/ionomycin for 4 hours. (**A**–**G**) n = 3–5 mice per group. Experiments were repeated 3 to 4 times. No txp, no transplant. Student's t test. (**H**) Marilyn T cell–CFSE dilution after culture as in **F** with male APCs from different groups. APCs were harvested 7 days after gavage of GF mice. Quantitation of divided Marilyn T cells (**I**) and IFN-γ production after restimulation (**J**). n = 2–8. One-way ANOVA. Data represent the mean ± SEM. $^*P < 0.05$; $^{**}P < 0.01$; $^{***}P < 0.001$.

(APCs), or both. To determine whether the Abx pretreatment affected APCs, we isolated T cell– and NK cell–depleted APCs from the skin dLNs of Abx-pretreated or control SPF male mice and used them to stimulate CFSE-labeled Marilyn T cells from naive mice in vitro. APCs from Abx-treated mice stimulated Marilyn T cells less vigorously than control APCs (Figure 3F). Marilyn T cell proliferation was also reduced when stimulated with H-Y peptide–pulsed APCs from Abx-pretreated females (Figure 3F) when compared with peptide-pulsed APCs from untreated females, suggesting that the APC defect is unlikely to be at the antigen-processing level. Marilyn T cells stimulated with APCs from Abx-treated mice also produced less IFN-γ (Figure 3G). Differences in T cell–priming ability were not due to an alteration in the composition of skin dLN APCs after Abx treatment, as the proportion of B cells, CD11b+ cells, and CD11c+ DCs as well as subsets of CD103+, CD8α+, or Siglec-H+ DCs was comparable in control and Abx-treated mice (Supplemental Figure 3, A–D), with the exception of a reduction in CD11b+ DCs. Moreover, expression levels of CD40, PDL1, CD80, CD86, ICOSL, OX40L, and I-A^b were similar on DCs from Abx-pretreated and control mice (Supplemental Figure 3E). Thus, Abx treatment reduced the capacity of APCs to prime alloreactive T cells. In the gnotobiotic setting, skin dLN APCs from male GF and GF-Abx.F mice also induced less proliferation and IFN-γ production by Marilyn T cells than did APCs from SPF or GF-SPF.F mice (Figure 3, H–J). Together, these data argue against a direct effect of oral Abx on immune cells or skin grafts and suggest instead that Abx-sensitive taxa play a critical role in poising skin dLN APCs for alloreactive T cell priming.

Abx treatment downregulates the type I IFN pathway in DCs. Since DCs are the main APC subset that activates alloreactive H-Y–specific T cells (12), skin dLN CD11c+ DCs were sorted from control and 10-day–Abx–treated mice for gene expression profiling.

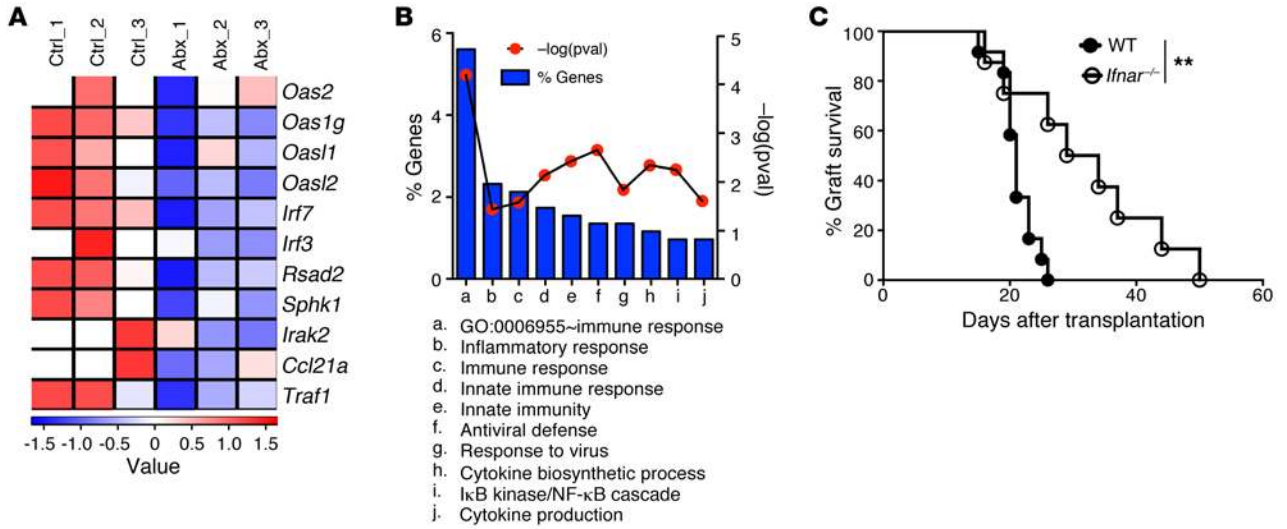

Figure 4. Abx pretreatment results in downregulation of the type I IFN pathway. (**A** and **B**) DCs from skin dLN of control and 10-day Abx-pretreated SPF mice were sorted, and cDNA was analyzed for gene expression profiling. (**A**) Examples of genes differentially expressed (n = 3 per group). (**B**) DAVID analysis of enriched pathways in DCs from control relative to Abx-treated groups. (**C**) Female B6 control and *Ifnar*$^{-/-}$ SPF mice were transplanted with skin grafts from males of the host genotype. Results are combined from 2 experiments. WT, n = 12; *Ifnar*$^{-/-}$, n = 8. log-rank test. $^{**}P < 0.01$.

DCs from Abx-treated mice displayed reduced expression of genes associated with the type I IFN pathway, such as IRF3, IRF7, OAS2, OAS1G, OASL1, and OASL2, as well as of genes related to activation of the NF-κB pathway, such as RSAD2, SPHK1, and IRAK2. In addition, genes involved in cytokine regulation and production were also significantly less expressed in DCs from Abx-treated than control mice (Figure 4, A and B). In keeping with this gene profiling analysis, survival of type I *Ifnar*-deficient male skin grafts was significantly prolonged in type I *Ifnar*-deficient females when compared with control mice (Figure 4C), supporting a role for type I IFN signaling in the response to H-Y^{+} skin grafts. IFN-αR expression had to be absent in both donor and recipient mice for graft survival to be prolonged (not shown). Notably, Abx pretreatment of *Ifnar*-deficient mice did not prolong survival compared with untreated counterparts; they were all rejected within 50 days (not shown), further suggesting that the effects of Abx pretreatment were dependent at least in part on a reduction of the type I IFN pathway.

Abx pretreatment also prolongs survival of major antigen–mismatched skin and MHC class II–mismatched cardiac allografts. It was conceivable that the effects of the microbiota on graft outcome were limited to the H-Y skin graft mouse model or applicable only to transplantation of colonized organs. To this end, donor and recipient mice were pretreated with Abx prior to transplantation of BALB/c skin or Bm12 heart into B6 animals. Abx pretreatment resulted in a significant delay in graft rejection in both models (Figure 5, A and B), arguing for a more generalizable effect of the microbiota on allograft rejection.

Discussion

Collectively, our results suggest that Abx pretreatment reduces the priming capacity of alloreactive T cells by skin dLN APCs, in part by impairing activation of the type I IFN pathway.

Our study demonstrates that bacterial communities existing in the fecal samples of untreated, but not Abx-pretreated, SPF mice can accelerate skin graft rejection after colonization of GF mice. This result underscores remarkable differences in the physiological effects of these bacterial communities based on their composition rather than their load and suggests that the Abx have eliminated species with key microbial products or metabolic functions for the priming of alloreactive T cells or enabled growth of inhibitory species. It is important to note that fecal gavage not only resulted in established intestinal species in the reconstituted GF mice, but also in colonization of their skin (Supplemental Figure 2A), presumably because the fur is in contact with soiled bedding in the gnotobiotic cages. Thus, it is yet unclear whether it is the microbial constituents of the intestine or of the skin that can promote alloreactivity. Indeed, defined skin commensals have recently been shown to modify local cutaneous immunity, affecting skin DCs and resident T cells and enhancing barrier immunity (13). The intestinal microbiota have also been shown to affect immunity as distal as the peripheral joints or the central nervous system in models of autoimmune arthritis or autoimmune encephalomyelitis (14, 15).

Gene expression profiling of DCs isolated from the LNs of Abx-pretreated mice revealed reduced expression of genes in the NF-κB and type I IFN pathways. These pathways have been previously associated with transplant rejection, as NF-κB inhibition in DCs with decoy oligodeoxyribonucleotides has been shown to promote allograft survival (16). Similarly, type I IFN therapy has been associated with liver rejection in the clinic (17), and viral and bacterial infections that induce a type I IFN response were reported to prevent the induction of transplantation tolerance (18–20). Peritoneal and splenic mononuclear phagocytes have been shown to require signals from the microbiota to elicit NK cell priming and antiviral immunity, including expression of type I IFN genes, and to promote an activating epigenetic transcriptional landscape for cytokine production (21, 22). Recent work from our group has identified select bacterial species within the *Bifidobac-*

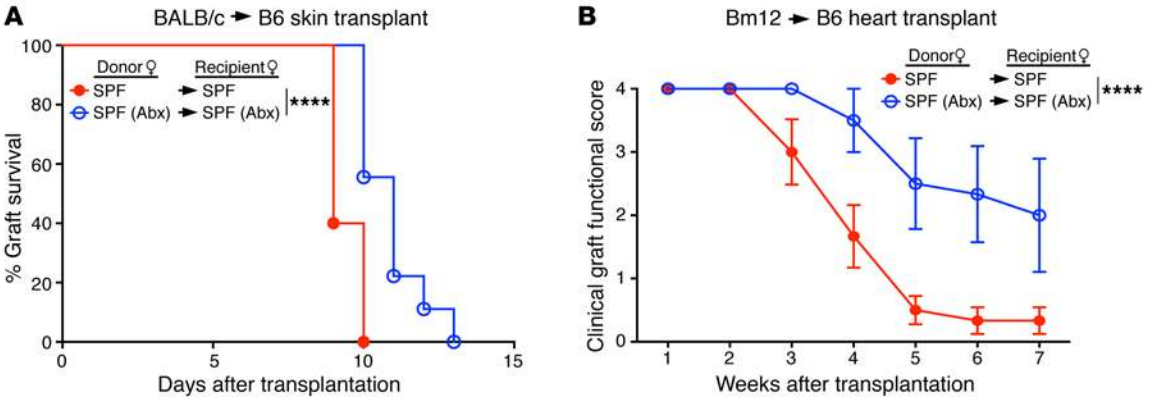

Figure 5. Abx pretreatment delays rejection of major antigen–mismatched skin and MHC class II–mismatched cardiac allografts. (**A**) Graft survival of BALB/c skin transplanted onto B6 recipients. Untreated, $n = 5$; Abx pretreatment, $n = 9$. log-rank test. (**B**) Clinical graft functional score of Bm12 heart transplanted into B6 recipients. $n = 6$ per group. Two-way ANOVA. Data represent the mean ± SEM. ****$P < 0.0001$.

terium genus capable of inducing the type I IFN pathway in DCs, resulting in improved tumor control (23). Our results indicate that the microbiota and type I IFN signaling promote rejection of H-Y$^+$ skin grafts and that Abx may eliminate bacterial species that normally poise skin dLN APCs for stimulation of alloreactive T cells or favor outgrowth of species that do not activate the type I IFN pathway in skin dLN APCs. Finally, the APC-poising effects are rapidly reversible, suggesting a continuous dialogue between the microbiota and the immune system, as APCs from SPF mice can lose their priming function upon a 10-day Abx treatment and APCs from GF mice can regain it upon 5- to 7-day exposure to fecal microbiota from control SPF but not Abx-pretreated mice.

These studies raise the question of which microbial-associated molecular patterns may be responsible for signaling to the skin dLN APCs to prepare them to stimulate T cells. The more extensive survival of male skin grafts by female hosts observed when both male donors and female recipients are deficient in MyD88 KO (4) compared with the effects of Abx pretreatment in our study suggests the possibility that both microbial and sterile inflammation ligands additively induce MyD88-dependent signaling following H-Y skin transplantation. Indeed, damage-associated molecules such as haptoglobin have been shown to contribute to the rejection of male skin grafts in a MyD88-dependent manner, with skin grafts from haptoglobin-deficient mice eliciting slower acute rejection than control skin grafts (24). In contrast, whether the prorejection effects of the microbiota are MyD88 dependent or not remains to be investigated. The fact that Abx pretreatment resulted in prolonged survival of fully MHC-mismatched allogeneic skin grafts in our study whereas rejection kinetics of major antigen–mismatched skin grafts were unmodified compared with controls when both donors and recipients lacked MyD88 (25) suggests that the microbiota may exert at least some of its effects in a MyD88-independent manner. Many pattern-recognition receptors can recognize microbial molecular patterns and signal in a MyD88-independent manner (26), including TLR3 and TLR4, NOD-like receptors, C-type lectin receptors, and sensors of intracellular DNA and RNA. Moreover, the microbiota can elaborate metabolic products that may have local or distal immune effects independently of the expression of pattern-recognition receptors. For instance, Clostridia can generate short-chain fatty acids that have been shown to promote intestinal Treg differentiation (7, 27–30). Thus, the microbial products capable of promoting allograft rejection and the sensors that recognize them need to be identified. In addition, whether immune cells are directly targeted by such microbial products or whether DCs are poised by signals elicited by intermediary cells such as mucosal or epidermal cells will need to be established. Our observation that Abx pretreatment can prolong survival of cardiac allografts, which are considered sterile, demonstrates distal effects of the microbiota, further suggesting that microbes, their products, or the local cells they instruct presumably circulate to sites of priming or effector function of alloreactive T cells. It is conceivable that incisions to the skin for any kind of surgery, including cardiac transplantation, may allow some cutaneous bacteria to enter the bloodstream and signal at distant sites and/or that intestinal bacterial translocation during open abdominal surgery, as occurs in our model of heterotopic cardiac transplantation, may contribute to the enhanced alloimmunity observed in colonized compared with GF animals. Indeed, portal endotoxin has been detected after abdominal surgery that did not involve intestinal sectioning (31).

The demonstration that the microbiota is an important environmental factor that continuously modulates the activation state of skin dLN APCs and their ability to prime alloreactive T cells points to the control of the composition of the microbiota as a potential therapeutic target to improve transplant outcomes.

Methods

Mice. Six-week-old SPF C57BL/6NHsd male and female mice were purchased from Envigo or bred in house. B6(C)-H2-Ab1^{bm12}/KhEgJ female mice were purchased from The Jackson Laboratory. CD45.1$^+$ *Rag2*-knockout (RAG-KO) Marilyn B6 mice whose CD4$^+$ T cells are specific for an H-Y antigen (32) were obtained from Charles Mainhart via Taconic Biosciences and bred in house under SPF conditions. *Ifnar*-KO mice were maintained in the University of Chicago animal facility. B6 GF mice were kept in plastic isolators at the University of Chicago's Gnotobiotic Research Animal Facility and were fed autoclaved food and water. Fecal aerobic and anaerobic cultures were carried out weekly to ensure the absence of microbial colonization.

Abx treatment. Eight-week-old B6 mice that had been cohoused to equilibrate their microbiota were divided into control and Abx treatment cages. Mice in Abx treatment cages received a daily gavage with 200 μl of Abx based on a previous report (7) containing gentamycin (0.35 mg/ml, Fresenius Kabi), kanamycin (5.25 mg/ml, Gibco, Thermo Fisher Scientific), colistin (8500 U, RPI), metronidazole (2.15 mg/ml, Sigma-Aldrich), and vancomycin (0.5 mg/ml, Hospira) diluted in autoclaved water. Abx were administered by daily gavage rather than in the drinking water to ensure accurate dosing. Donor and recipient mice were treated for 10 days until the time of transplantation.

Transplantation. For aseptic surgery for SPF mice, tail skin from male B6 or from BALB/c donor mice was transplanted onto the flank of female recipients. Bandages were removed after 7 days. Graft survival was monitored every other day, and the day at which less than 20% of viable skin tissue was left was called the day of rejection. For sterile surgery for gnotobiotic and SPF mice, sterile surgical techniques in a biological safety cabinet as previously described (8) were used. Bm12 hearts were transplanted into B6 mice as previously described (33). Because this is a chronic rejection model (34), clinical graft functional scores adapted from Tanaka et al. (35) were calculated as follows: heart size (small = 1, large = 0), speed of heartbeat (too fast to count = 3, 100–200 beats/min = 2, <100 beats/min = 1, heartbeat cessation = 0).

Leukocyte isolation. Spleen, or skin dLN (inguinal, axillary, and brachial) cells were isolated at the indicated times, resuspended in complete DMEM (Corning) with 10%FBS, 1% penicillin/streptomycin, 1% L-glutamine, 1% NEAA, 1% HEPES, and 0.028 mM β-mercaptoethanol, and counted using a Countess cell counter. For skin leukocyte isolation, skin grafts or shaved flank was harvested. The skin was cut into small pieces, resuspended in RPMI (Corning) medium supplemented with Liberase (0.4 mg/ml, Roche) and DNAse (0.01%, MP Biomedicals), and incubated for 2 hours at 37°C. After incubation, the skin was homogenized using a 70-μm cell strainer, a petri dish, and a syringe plunger. Single-cell suspensions were centrifuged, and pellets were resuspended in complete RPMI medium before cells were counted.

In vitro stimulation of graft-infiltrating cells. Isolated graft-infiltrating cells (5×10^6) were plated in 6-well tissue culture plates. PMA (50 ng/ml), ionomycin (0.5 μg/ml), and brefeldin A (5 μg/ml) were added into each well, and cells were incubated for 4 hours at 37°C in 8% CO_2. Stimulated cells were harvested for staining and flow cytometry analysis.

CFSE labeling. CD45.1$^+$ RAG-KO CD4$^+$ Marilyn T cells were collected from peripheral LNs and spleen. Red blood cells in spleens were lysed with ACK lysis buffer for 5 minutes. Cells from LNs and spleen were combined, counted, and resuspended at a concentration of 20×10^6 cells/ml in serum-free DMEM. CFSE (C34554, Life Technologies) was diluted to a final concentration of 5 μM and incubated with cells for 10 minutes at 37°C. Labeling was stopped with an equal volume of fetal bovine serum. Cells were centrifuged and resuspended in complete DMEM. For adoptive transfer, the cells were washed and resuspended in 1× PBS.

Adoptive transfer of Marilyn T cells. CFSE-labeled CD45.1$^+$ RAG-KO CD4 Marilyn T cells (1×10^6) were transferred i.v. into B6 mice 1 day prior to skin transplantation. At day 4 after transplantation, skin dLNs (brachial and axillary) were harvested and isolated leukocytes stained to assess T cell proliferation.

Ex vivo stimulation of Marilyn T cells. APCs were isolated from skin dLNs of male or female B6 mice following magnetic enrichment with biotinylated anti-Thy1.2 (53-2.1, eBioscience) and anti-NK1.1 (Frank W. Fitch Monoclonal Antibody Facility, University of Chicago) antibodies. Marilyn T cells were magnetically enriched from the peripheral LNs and spleens of Marilyn mice using streptavidin magnetic beads (catalog 88817, Pierce), anti–Ter119-biotin (TER-119, eBioscience), anti–CD11b-biotin (M1/70, eBioscience), and anti–NK1.1-biotin (PK136, Frank W. Fitch Monoclonal Antibody Facility at the University of Chicago) prior to CFSE labeling. APCs ($1–2 \times 10^5$/well) were cultured in triplicate with Marilyn T cells (1×10^5/well) in complete DMEM for 3 days. T cells were restimulated with PMA (50 ng/ml) and ionomycin (0.5 μg/ml) in the presence of brefeldin A (5 μg/ml) for 4 hours at 37°C and analyzed by flow cytometry. For stimulation with female APCs, the culture was supplemented with 1 to 20 pM of CD4 H-Y peptide (NAGFNSNRANSSRSS), which was synthesized by Joel Collier (University of Chicago).

Flow cytometry. All cells were stained with 1:1000 Live Aqua Live/Dead stain (Life Technologies) prior to phenotypic staining. For graft-infiltrating cell analyses, cells were stained with anti–CD45.2-APC (104, eBioscience), anti–TCR-β–PerCP Cy5.5 (H57597, eBioscience), anti–CD4-PE-Cy7 (RM4-5, eBioscience), anti–CD8α-eF450 (53-6.7, eBioscience), and anti–TCR-γδ–PE (eBioGL3, eBioscience). For cell population analyses, cells were stained with anti–CD45.2-APC (104, eBioscience), anti–TCR-β–PerCP Cy5.5 (H57597, eBioscience), anti–CD19-FITC (eBio1D3, eBioscience), anti–CD4-BV605 (RM4-5, BioLegend), anti–CD8α-BV711 (53-6.7, BioLegend), anti–NK1.1-PE (PK136, BD Biosciences — Pharmingen), anti–CD11c-PECy7 (N418, eBioscience), anti–CD11b-APC-Cy7 (M1/70, eBioscience), and anti–Gr-1–AF700 (RB6-8C5, eBioscience). For adoptive transfer and in vitro stimulation analyses, cultured cells were stained with anti–CD45.1-APC-eF780 (A20, eBioscience), anti–CD45.2-APC (104, eBioscience), anti–TCR-β–PerCP–Cy5.5 (H57597, eBioscience), anti–CD4-PE-Cy7 (RM4-5, eBioscience), and anti–IFN-γ–PE (XMG1.2, eBioscience). For intracellular cytokine staining, cells were fixed with 1% formaldehyde for a 10-minute incubation at 37°C, followed by cold 1× PBS and methanol treatment overnight. Fixed and permeabilized cells were stained with antibodies. All samples were analyzed with the LSR Fortessa (BD Biosciences).

Fecal reconstitution. Fresh fecal pellets from untreated or Abx-treated female mice were resuspended in 1 ml of sterile PBS. GF mice were reconstituted by oral gavage with 200 μl of such suspension 5 to 7 days before skin transplantation. The status of fecal and cutaneous colonization was analyzed at different time points using quantitative PCR (qPCR) for bacterial load and presence of select bacterial taxa.

DNA extraction. Fecal samples were homogenized with 0.1 mm zirconia/silica beads in 1.4 ml ASL buffer (51504, QIAGEN) in a MiniBeadbeater (Biospec). DNA was extracted with the QIAamp DNA Stool Mini Kit (51504, QIAGEN). Tail skin samples were incubated in enzymatic lysis buffer (20 mM Tris, 2 mM EDTA, 1.2% Triton X-100, pH 8.0) and lysozyme (20 mg/ml) for 3 hours at 37°C. Standard protocols for DNA purification of MasterPure Yeast DNA Purification Kit (MPY80200, Epicentre Biotechnologies) and QIAamp DNA Stool Mini Kit (51504, QIAGEN) were followed for all subsequent steps.

16S rRNA gene sequencing and data analysis. 16S rRNA genes were amplified from purified DNA using PCR primers (F515/R806) specific for the V4–V5 region of the 16S rRNA gene and sequenced by

Illumina MiSeq at the High-Throughput Genome Analysis Core in the Argonne National Laboratory, Argonne, Illinois, USA), using previously described sequencing primers (36). Quantitative Insights Into Microbial Ecology (QIIME) software (37) was used for de novo operational taxonomic unit (OTU) selection (with 97% identity threshold), rarefaction, and taxonomic classification. Microbial communities were compared using the unweighted UniFrac distance metric (38) and were displayed using PCA plots. The data were uploaded to the European Nucleotide Archive (ENA PRJEB13722).

qPCR for bacterial load and taxa assays. Bacterial load of extracted fecal DNA was determined by qPCR with the universal primers 8F and 338R for the 16S rRNA gene, using iQ SYBR Green Supermix (Bio-Rad Life Science) and the 7300 Real-Time PCR system (Applied Biosystems). DNA was quantified against a standard curve as described (7), and the results were normalized to the weight of fecal samples. For taxa assays, the following primers were used: *B. coccoides,* forward, 5′-ACTCCTACGGGAGGCAGC-3′, reverse, 5′-GCTTCTTAGTCAGGTACCGTCAT-3′; *Lactobacillus* spp., forward, 5′-AGCAGTAGGGAATCTTCCA-3′, reverse, 5′-CACCGCTACACATGGAG-3′. Data acquisition and analysis were done using iQ SYBR Green Supermix (Bio-Rad Life Science) and the 7300 Real-Time PCR system (Applied Biosystems).

Gene array of DCs. The inguinal, brachial, and axillary LNs were minced with a razor blade, treated with 400 U of Collagenase IV (Sigma-Aldrich) and 0.01% DNase (MP Biomedicals), and incubated at 37°C for 30 minutes, followed by homogenization with a syringe plunger and 40-μM filters. Cells were stained with 1:1000 Live Aqua LIVE/DEAD stain (Life Technologies), anti–NK1.1-BV421 (PK136, BioLegend), anti–CD19-BV421 (6D5, BioLegend), anti–TCRβ-BV421 (H57-597, BD Horizon), and anti–I-A^b-PE (AF6-120.1, BD Biosciences — Pharmingen) and sorted into RLT buffer (QIAGEN) using the BD FACS Aria II (BD Biosciences). DCs were sorted in RLT buffer from the RNeasy Micro Kit (QIAGEN). RNA was isolated according to the manufacturer's protocol and analyzed at the University of Chicago Genomics Core facility. RNA integrity and concentration were assessed using Agilent Bioanalyzer 2100. RNA with an RNA integrity number greater than 9.0 was processed into cRNA and hybridized to the Illumina MouseRef-8 v2 array using the manufacturer's protocol and scanned in Illumina HiScan. Quantile normalized and background-subtracted values were analyzed using R version 3.2.0. Genes with an expression value under 25 were removed from the analysis. Mean fold change in expression level between control and Abx DCs was calculated. Genes with a fold change of 1.5 were analyzed on the Database for Annotation, Visualization and Integrated Discovery (DAVID; NIH) v6.7 for pathway analysis. Genes that were significantly enriched in the pathway analysis ($P < 0.05$) were chosen and plotted in a heat map using R. All original microarray data were deposited in the NCBI's Gene Expression Omnibus (GEO GSE80487).

Statistics. Graft survival curves were analyzed using Kaplan-Meier plots and log-rank post hoc tests. Comparisons between control and Abx samples for Shannon index, T cell populations, Marilyn T cell division, and cytokine production were analyzed with 2-tailed unpaired *t* test. Analysis of DC subsets and costimulatory molecules was performed with 2-way ANOVA. Multiple comparisons among control Abx, GF, GF-SPF.F, and GF-Abx.F samples were done with 1-way ANOVA, together with Bonferroni's comparison. *P* values of less than 0.05 were considered to be statistically significant. Statistical analysis was performed using Graphpad Prism 6.

Study approval. Mouse studies were approved by the Animal Resources Center of the University of Chicago under IACUC guidelines (protocol 71095) and according to the NIH guidelines for animal use.

Author contributions

YML, LC, LLM, CB, ASC, and MLA designed the study. BT, CB, LC, and YW developed the sterile surgical technique for skin grafting GF mice in a biosafety cabinet. YML, LC, and CB conducted in vivo, ex vivo, and in vitro experiments and analyzed the data. LC, YW, and CB performed microsurgery and monitored skin graft survival. ATS and CRN provided experimental advice and technical support on microbiome analyses. KAM, ASS, and TFG contributed to analysis of gene expression profiling. YML and MLA wrote the manuscript, and all authors contributed to editing it.

Acknowledgments

This work was supported by National Institute of Allergy and Infectious Diseases (NIAID) grants P01AI-97113 to A.S. Chong and M.L. Alegre; R01 AI071080 to M.L. Alegre; ROTRF 979162997 and NIAID RO1 AI106302 to C.R. Nagler; and NIAID R01 AI072630 to A.S. Chong. We thank Lekha Nair for help with experiments, Taylor Feehley for help with the initiation of this project, Joel Collier for the synthesis of the CD4 H-Y peptide, Alan Vest for help with gnotobiotic husbandry, and the University of Chicago Research Computing Center for support with computational resources.

Address correspondence to: Maria-Luisa Alegre, 924 E. 57th St., JFK-R312, Chicago, Illinois 60637, USA. Phone: 773.834.4317; E-mail: malegre@midway.uchicago.edu.

1. Ahmed EB, Wang T, Daniels M, Alegre ML, Chong AS. IL-6 induced by Staphylococcus aureus infection prevents the induction of skin allograft acceptance in mice. *Am J Transplant*. 2011;11(5):936–946.
2. Wang T, et al. Infection with the intracellular bacterium, Listeria monocytogenes, overrides established tolerance in a mouse cardiac allograft model. *Am J Transplant*. 2010;10(7):1524–1533.
3. Belkaid Y, Hand TW. Role of the microbiota in immunity and inflammation. *Cell*. 2014;157(1):121–141.
4. Goldstein DR, Tesar BM, Akira S, Lakkis FG. Critical role of the Toll-like receptor signal adaptor protein MyD88 in acute allograft rejection. *J Clin Invest*. 2003;111(10):1571–1578.
5. Oh PL, Martinez I, Sun Y, Walter J, Peterson DA, Mercer DF. Characterization of the ileal microbiota in rejecting and nonrejecting recipients of small bowel transplants. *Am J Transplant*. 2012;12(3):753–762.
6. Charlson ES, et al. Lung-enriched organisms and aberrant bacterial and fungal respiratory microbiota after lung transplant. *Am J Respir Crit Care Med*. 2012;186(6):536–545.
7. Stefka AT, et al. Commensal bacteria protect against food allergen sensitization. *Proc Natl Acad Sci U S A*. 2014;111(36):13145–13150.
8. Theriault B, Wang Y, Chen L, Vest A, Bartman C, Alegre ML. Long-term maintenance of sterility following skin transplantation in germ-free mice. *Transplant Direct*. 2015;1(8):e28.
9. Itoh K, Mitsuoka T. Characterization of clostridia isolated from faeces of limited flora mice and their effect on caecal size when associated with germ-free mice. *Lab Anim*. 1985;19(2):111–118.
10. Liu C, Finegold SM, Song Y, Lawson PA. Reclassification of Clostridium coccoides, Ruminococcus hansenii, Ruminococcus hydrogenotrophicus,

Ruminococcus luti, Ruminococcus productus and Ruminococcus schinkii as Blautia coccoides gen. nov., comb. nov., Blautia hansenii comb. nov., Blautia hydrogenotrophica comb. nov., Blautia luti comb. nov., Blautia producta comb. nov., Blautia schinkii comb. nov. and description of Blautia wexlerae sp. nov., isolated from human faeces. *Int J Syst Evol Microbiol*. 2008; 58(pt 8):1896–1902.
11. Reed AJ, et al. Alloreactive CD4 T cell activation in vivo: an autonomous function of the indirect pathway of alloantigen presentation. *J Immunol*. 2003;171(12):6502–6509.
12. Atif SM, et al. Cutting Edge: roles for Batf3-dependent APCs in the rejection of minor histocompatibility antigen-mismatched grafts. *J Immunol*. 2015;195(1):46–50.
13. Naik S, et al. Commensal-dendritic-cell interaction specifies a unique protective skin immune signature. *Nature*. 2015;5(7545):104–108.
14. Lee YK, Menezes JS, Umesaki Y, Mazmanian SK. Proinflammatory T-cell responses to gut microbiota promote experimental autoimmune encephalomyelitis. *Proc Natl Acad Sci U S A*. 2011;108(suppl 1):4615–4622.
15. Wu HJ, et al. Gut-residing segmented filamentous bacteria drive autoimmune arthritis via T helper 17 cells. *Immunity*. 2010;32(6):815–827.
16. Giannoukakis N, et al. Prolongation of cardiac allograft survival using dendritic cells treated with NF-κB decoy oligodeoxyribonucleotides. *Mol Ther*. 2000;1(5 pt 1):430–437.
17. Stravitz RT, et al. Effects of interferon treatment on liver histology and allograft rejection in patients with recurrent hepatitis C following liver transplantation. *Liver Transpl*. 2004;10(7):850–858.
18. Cook CH, et al. Disruption of murine cardiac allograft acceptance by latent cytomegalovirus. *Am J Transplant*. 2009;9(1):42–53.
19. Stapler D, et al. Expansion of effector memory TCR Vβ4$^+$ CD8$^+$ T cells is associated with latent infection-mediated resistance to transplantation tolerance. *J Immunol*. 2008;180(5):3190–3200.
20. Wang T, et al. Prevention of allograft tolerance by bacterial infection with Listeria monocytogenes. *J Immunol*. 2008;180(9):5991–5999.
21. Ganal SC, et al. Priming of natural killer cells by nonmucosal mononuclear phagocytes requires instructive signals from commensal microbiota. *Immunity*. 2012;37(1):171–186.
22. Abt MC, et al. Commensal bacteria calibrate the activation threshold of innate antiviral immunity. *Immunity*. 2012;37(1):158–170.
23. Sivan A, et al. Commensal Bifidobacterium promotes antitumor immunity and facilitates anti-PD-L1 efficacy. *Science*. 2015;350(6264):1084–1089.
24. Shen H, et al. Haptoglobin activates innate immunity to enhance acute transplant rejection in mice. *J Clin Invest*. 2012;122(1):383–387.
25. Tesar BM, Zhang J, Li Q, Goldstein DR. TH1 immune responses to fully MHC mismatched allografts are diminished in the absence of MyD88, a toll-like receptor signal adaptor protein. *Am J Transplant*. 2004;4(9):1429–1439.
26. Brubaker SW, Bonham KS, Zanoni I, Kagan JC. Innate immune pattern recognition: a cell biological perspective. *Annu Rev Immunol*. 2015;33:257–290.
27. Atarashi K, et al. Treg induction by a rationally selected mixture of Clostridia strains from the human microbiota. *Nature*. 2013;500(7461):232–236.
28. Arpaia N, et al. Metabolites produced by commensal bacteria promote peripheral regulatory T-cell generation. *Nature*. 2013;13(7480):451–455.
29. Furusawa Y, et al. Commensal microbe-derived butyrate induces the differentiation of colonic regulatory T cells. *Nature*. 2013;13(7480):446–450.
30. Smith PM, et al. The microbial metabolites, short-chain fatty acids, regulate colonic Treg cell homeostasis. *Science*. 2013;341(6145):569–573.
31. Abdala E, et al. Bacterial translocation during liver transplantation: a randomized trial comparing conventional with venovenous bypass vs. piggyback methods. *Liver Transpl*. 2007;13(4):488–496.
32. Perez-Diez A, et al. CD4 cells can be more efficient at tumor rejection than CD8 cells. *Blood*. 2007;109(12):5346–5354.
33. Corry RJ, Winn HJ, Russell PS. Primarily vascularized allografts of hearts in mice. The role of H-2D, H-2K, and non-H-2 antigens in rejection. *Transplantation*. 1973;16(4):343–350.
34. Yuan X, et al. A novel role of CD4 Th17 cells in mediating cardiac allograft rejection and vasculopathy. *J Exp Med*. 2008;1(13):3133–3144.
35. Tanaka M, et al. In vivo visualization of cardiac allograft rejection and trafficking passenger leukocytes using bioluminescence imaging. *Circulation*. 2005;112(9 suppl):I105–I110.
36. Caporaso JG, et al. Ultra-high-throughput microbial community analysis on the Illumina HiSeq and MiSeq platforms. *ISME J*. 2012;6(8):1621–1624.
37. Caporaso JG, et al. QIIME allows analysis of high-throughput community sequencing data. *Nat Methods*. 2010;7(5):335–336.
38. Lozupone C, Knight R. UniFrac: a new phylogenetic method for comparing microbial communities. *Appl Environ Microbiol*. 2005;71(12):8228–8235.